

Submitted to both student and technical conference

A Predictive Code for International Space Station Radiation Mission Planning

S. El-Jaby¹, B. Lewis¹, L. Tomi²

¹Royal Military College of Canada, Kingston, Ontario, Canada

²Canadian Space Agency, Saint-Hubert, Quebec, Canada

Abstract

A model developed for radiation mission planning aboard the International Space Station (ISS) is presented. The model utilizes a correlation between the ambient dose equivalent rate determined by a tissue equivalent proportional counter (TEPC) aboard the ISS and the cut-off rigidity parameter estimated from ISS position vectors. A preliminary assessment indicates the model can predict the total ambient dose equivalent to within 20% of tabulated measurements.

1. Introduction

A primary component of space mission planning aboard the International Space Station (ISS) is the accurate assessment of the radiation exposure that crew will experience for the duration of the mission. An accurate characterization of absorbed dose is paramount to crew safety and will dictate the longevity of crew careers. There have been several predictive models employed to estimate crew exposures during planned missions. Such models include the National Aeronautics and Space Administration's (NASA) high-charge-and-energy transport computer program (HZETRN), baryon transport code (BRNTRN), galactic heavy ion transport code (GCRTRN), proton dose code (PDOSE) [1], and extra-vehicular activities exposure estimation tool (EVADOSE) [2]. Other models include the Belgian Institute for Space Aeronautics' SHIELDOSE program [1] and the European Space Agency's DESIRE program [3,4]. The common theme among these models is that they rely on the use of particle flux models to describe the space radiation environment in low-Earth orbit. Such models include the AP-8 and AE-8 trapped radiation environment models for protons and electrons [5], respectively, and the Cosmic Ray Effects on Micro-Electronics (CREME) code describing the galactic cosmic radiation environment [6]. AP-8 and AE-8 utilize data collected from various satellites and detectors from the late 1950s to the early 1970s while CREME was last updated in 1996 [5,6]. On account of Earth's changing magnetic field conditions, however, these particle flux models have become increasingly less accurate with time [5].

The ISS international partners have developed various personal and area dosimeters employed to measure the exposure aboard the ISS. Based on a review of the relevant literature, it is believed that the data collected by these detectors have never been utilized in any predictive dose model thus far. The work presented here details preliminary results towards the development of a predictive model that will utilize, as its basis, an empirically developed relationship between the ambient dose equivalent rate measured by a US tissue equivalent proportional counter (TEPC) and the cut-off rigidity parameter interpolated from ISS position vectors. Unlike previous and currently employed codes, the model proposed here will eliminate the need for continuously updating the extremely complex particle flux spectrum of low-Earth orbit. Instead, it will only require an updated version of the cut-off rigidity map. Such updates are regularly produced [7].

2. Background

The International Space Station operates in low-Earth orbit (LEO) at an orbital inclination of approximately 51.6° . Over time, the ISS can range in altitude from approximately 300 km to approximately 500 km. Each orbit takes roughly 90 minutes to complete. The sources of radiation in LEO include galactic cosmic radiation (GCR), trapped radiation, solar particle events (SPEs), and albedo neutrons arising from ionic interactions with Earth's atmosphere [8-11].

2.1. Space radiation environment in low-Earth orbit

Galactic cosmic radiation originates from outside the solar system and consists of ~90% protons, ~7-10% helium nuclei, and ~1% heavier nuclei ranging from carbon to iron. GCR can reach kinetic energies of 10^{20} eV [8-11]. The inner trapped radiation belt (or inner Van Allen Belt) holds high energy protons of 50 MeV and electrons of energy greater than 30 MeV [8-11]. Galactic cosmic radiation and trapped radiation exposures each account for approximately half of the absorbed dose that crew will face. Exposures resulting from trapped radiation in LEO only occur when the ISS passes through the South Atlantic Anomaly (SAA). Outside this region, radiation exposures result predominantly from GCR [10]. Solar energetic particles (SEPs) arise from occasional disturbances in the Sun including solar flares and coronal mass ejections. It is difficult to predict the intensity and occurrence of SEPs, however within hours of onset, the particle flux of high energy protons reaching Earth can increase two to five times above typical levels and may last from hours to days. Consequently, SEPs may increase the level of exposure [10].

On account of the magnetosphere, the ability of charged ions to penetrate to a given position about the Earth changes with altitude, latitude, and longitude. This penetration ability is typically quantified by the cut-off rigidity parameter R_c . The rigidity of a particle is its ratio of momentum to charge and is given in units of GV. The cut-off rigidity indicates the minimum momentum needed by a charged particle to penetrate to a given position about the Earth. The cut-off rigidities about the Earth are strongly dependent on magnetic field fluctuations. Furthermore, they are dynamic in that they change as Earth's internal magnetic field changes and, in the short term, fluctuate with solar particle events [12-16]. Also, the amount of radiation exposure from GCR and trapped radiation has been shown to be anti-coincident with the level of solar activity [10,16,17]. The Sun will typically follow an eleven year solar modulation cycle. During periods of maximum solar activity, the amount of solar wind emanating from the sun will be relatively greater than during periods of minimum solar activity. The increased solar activity will act as a barrier to GCR thus reducing GCR exposure. Moreover, the increase in ultraviolet radiation will increase proton loss within the trapped radiation belts through atmospheric expansion and similarly reduce trapped radiation exposure [8,10,11].

2.2. Tissue equivalent proportional counter

The Space Radiation Analysis Group (SRAG) of NASA has been operating the US tissue equivalent proportional counter (TEPC) aboard the ISS from the year 2000 to the present time [18]. The data that the TEPC has been collecting over this period is well correlated with the descending phase of Solar Cycle 23 from near solar maximum to near solar minimum. Operationally, the TEPC is capable of measuring the mixed radiation field observed in LEO (i.e.,

low and high linear energy transfer radiation types) and from these measurements will provide an estimate of the absorbed dose rate $\dot{D}(\mu\text{Gy} \cdot \text{min}^{-1})$ and ambient dose equivalent $\dot{H}_{\text{TEPC}}^*(\mu\text{Sv} \cdot \text{min}^{-1})$ [9,11,19]. SRAG operates the TEPC to take and transmit measurements on a by-minute basis throughout each orbital pass of the ISS. For each dose measurement, an associated ISS position vector with respect to time (year, month, day, hour, minute, second), latitude, longitude, and altitude is recorded. SRAG, furthermore, records the TEPC placement aboard the ISS and utilizes a dose threshold procedure to account for exposures resulting from GCR sources, trapped radiation sources, and SEPs. These data are archived by SRAG and updated in real-time through their share-point website [18].

3. Model development

3.1. Raw data used

3.1.1. Tissue equivalent proportional counter data

The Space Radiation Analysis Group has provided two sets of TEPC data taken during July 7-13, 2001 and December 10-16, 2008. The data represent near solar maximum conditions and near solar minimum conditions, respectively, of Solar Cycle 23. A sample excerpt of the TEPC data is shown in Table 1 [18]. At a given minute, the dose rate and ambient dose equivalent rate are listed, as is the ISS position vector. The radiation type indicates the exposure source as determined by SRAG. Both data sets were taken with the TEPC placed in ISS service module panel 327 (SM-327).

Table 1. Excerpt of TEPC data collected on 12/10/2008 [18].

Date	Ambient Dose	Ambient Dose Equivalent	Longitude	Latitude	Altitude	Radiation Type
(GMT)	($\mu\text{Gy min}^{-1}$)	($\mu\text{Sv min}^{-1}$)	(deg.)	(deg.)	(km)	
.....
12/10/2008 00:04:13	0.029	0.046	-65.309	0.581	355.033	GCR
12/10/2008 00:05:13	0.037	0.179	-63.119	-2.519	355.775	GCR
12/10/2008 00:06:13	0.034	0.047	-60.919	-5.614	356.614	Trapped
12/10/2008 00:07:13	0.069	0.421	-58.693	-8.698	357.547	Trapped
.....

3.1.2. Cut-off rigidity map

The ISS position vectors (latitude, longitude) are interpolated over two world-grid estimates of the cut-off rigidity. These estimates include: (i) the effective vertical cut-off rigidity for 2001 at an altitude of 400 km generated by the Smart and Shea RCINTUT3 cut-off rigidity code [20] (see Fig. 1) and (ii) an effective vertical cut-off rigidity map utilizing the IGRF-2005 internal magnetic source developed by Nymmik et al. [21] for an altitude of 400 to 450 km.

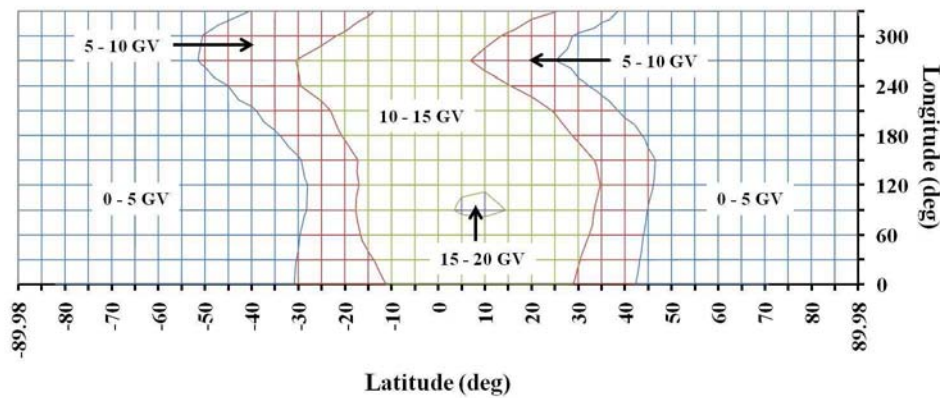


Figure 1. Smart and Shea RCINTUT3 cut-off rigidity map for year 2001 and 400 km altitude [20].

3.1.3. South Atlantic Anomaly

A proton flux map produced by Ginot et al. for the epoch of 2001 to 2006 and altitude of 400 to 450 km was used to define the SAA [22]. The proton flux map was digitized into upper and lower boundaries (see Fig. 2). Within the limits of the SAA, exposures result from trapped radiation sources. Outside the SAA, exposures result from GCR sources.

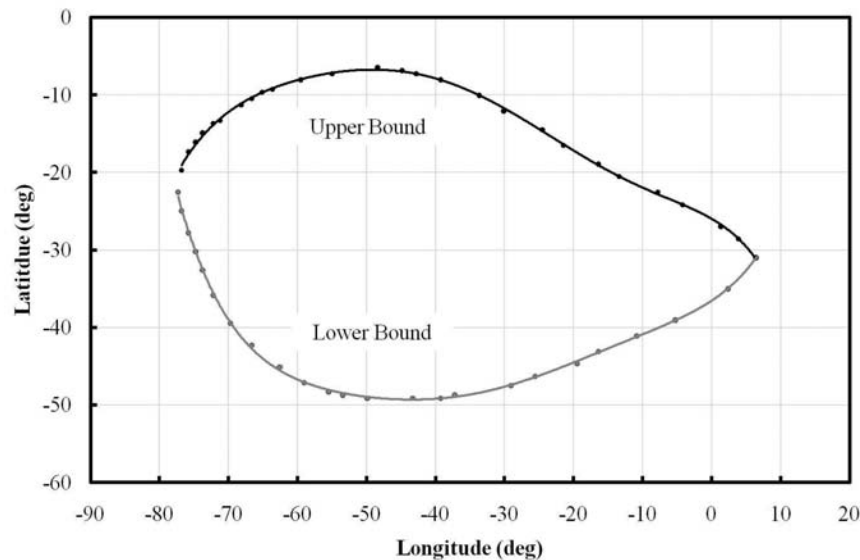


Figure 2. South Atlantic Anomaly geographical demarcation.

3.1.4. Solar modulation effects

The TEPC data used represent solar maximum and solar minimum conditions. To predict the ambient dose equivalent rate during moderate solar activity, three commonly used solar modulation parameters are used to provide the measure of activity. These parameters include the

12 month running mean of the international sunspot number (SSN) [23], the solar radio flux at 10.7 cm wavelength (F10.7cm) in solar flux units (s.f.u) [23], and the heliocentric potential U (GV) [24]. The values in Table 2 list the monthly values of the three parameters for July 2001 (solar maximum) and December 2008 (solar minimum). From these extremes, a linear interpolation can be performed to scale the ambient dose equivalent rates to the correct level of solar modulation.

Table 2. Solar modulation parameters: 12 month running mean sun-spot number (SSN) [23], solar radio flux (F10.7cm) [23], and heliocentric potential (U) [24].

Solar Modulation Parameters	Minimum Value	Maximum Value
SSN	1.7	111.7
F10.7cm (s.f.u)	69.05	131.72
U (GV)	266	773

3.2. Parametric fit development

The ISS position vectors are linearly interpolated against the cut-off rigidity maps discussed in Section 3.1.2 to obtain corresponding cut-off rigidity values. The July 7-13, 2001 TEPC data set is interpolated against the Smart and Shea cut-off rigidity map for 2001. The IGRF-2005 Nymmik cut-off rigidity map is utilized as the best approximation to the December 10-16, 2008 TEPC data set. The ambient dose equivalent rate \dot{H}_{TEPC}^* ($\mu\text{Sv min}^{-1}$) versus cut-off rigidity R_c (GV) data are then parsed into the type of radiation source causing the exposure (GCR, SPE, Trapped). A regression analysis on the parsed, raw data was performed. Best fit curves were obtained for GCR exposures, given by Eq. (1), and for trapped radiation exposures, given by Eq. (2). There were no instances of SEPs in the data set. The curve-fit parameters determined by regression are listed in Table 3. The bracketed values are the 95% confidence limits of the regression fit parameters.

$$\dot{H}_{TEPC/GCR}^* = a_1 e^{-\frac{R_c}{b_1}} \quad (1)$$

$$\dot{H}_{TEPC/Trap}^* = a_2 e^{-0.5\left(\frac{R_c-b_2}{c_2}\right)^2} \quad (2)$$

Table 3. Regression parameters for Eqs. (1) and (2). Bracketed values are the lower and upper 95% confidence limits on the regression fit parameters. Values are rounded to three decimal places.

Curve-Fit Parameters	Solar Maximum	Solar Minimum
a_1	0.647 (0.636/0.657)	0.924 (0.911/0.936)
b_1	6.186 (6.018/6.353)	4.528 (4.435/4.621)
a_2	4.238 (3.769/4.708)	6.924 (6.304/7.543)
b_2	7.378 (7.139/7.618)	7.460 (7.295/7.624)
c_2	1.914 (1.666/2.161)	1.673 (1.505/1.841)

Figures 3 to 6 illustrate the best fit curves for GCR exposures and trapped radiation exposures, respectively, for solar maximum and solar minimum conditions.

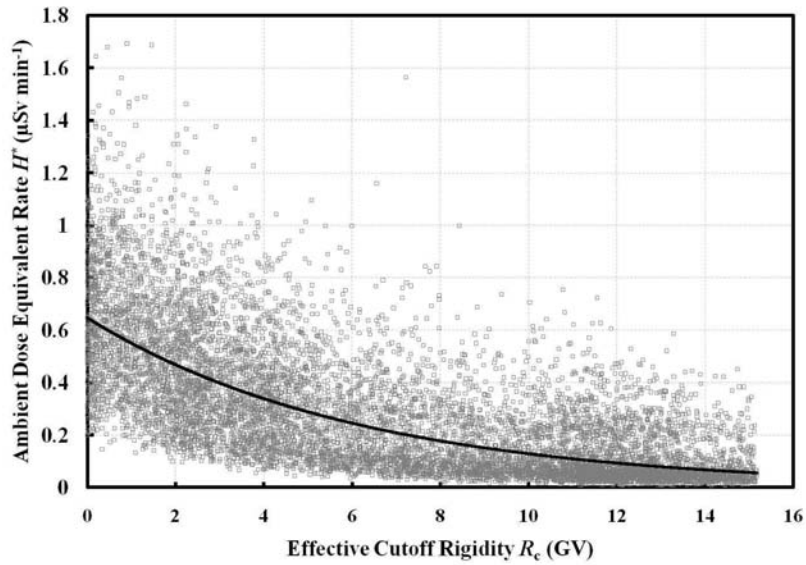


Figure 3. GCR exposure parametric fit for July 7-13, 2001 (solar maximum) TEPC data set interpolated against Smart and Shea 2001 cut-off rigidity map.

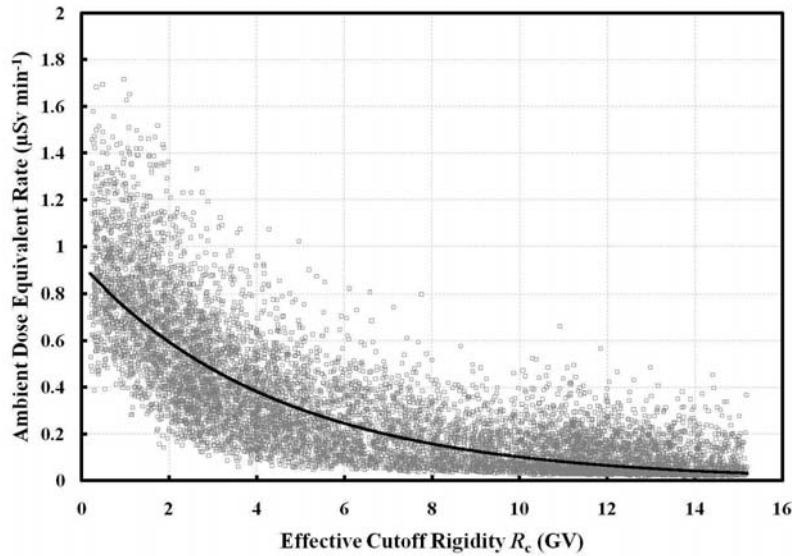


Figure 4. GCR exposure parametric fit for December 10-16, 2008 (solar minimum) TEPC data set interpolated against IGRF-2005 cut-off rigidity map introduced by Nymmik et al.

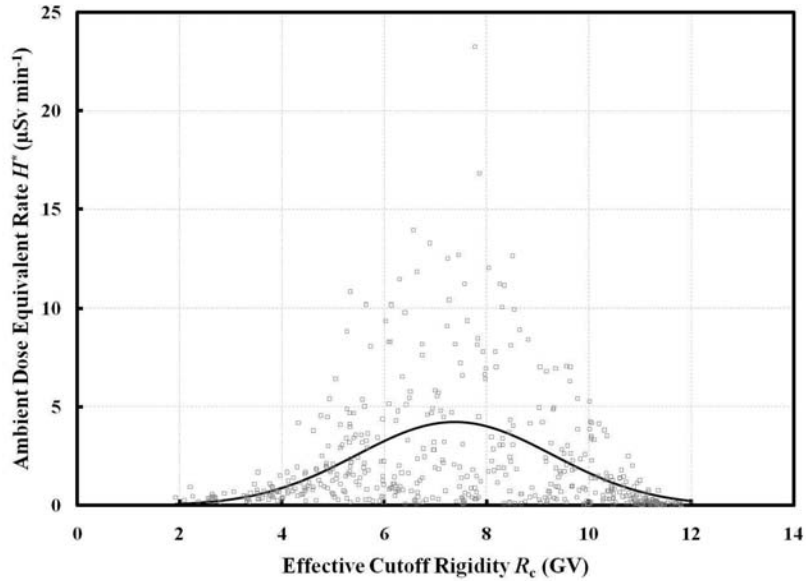


Figure 5. Trapped radiation exposure parametric fit for July 7-13, 2001 (solar maximum) TEPC data set interpolated against Smart and Shea 2001 cut-off rigidity map.

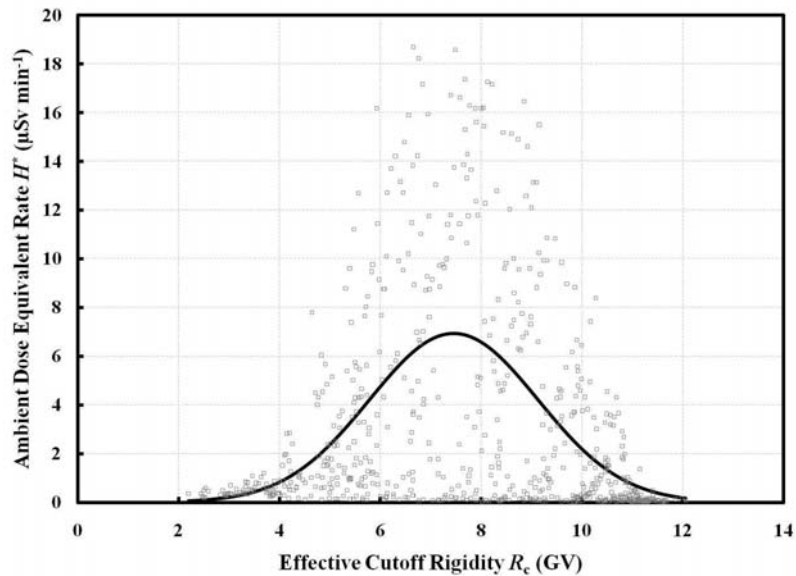


Figure 6. Trapped radiation exposure parametric fit for December 10-16, 2008 (solar minimum) TEPC data set interpolated against IGRF-2005 cut-off rigidity map introduced by Nymmik et al.

Figures 7 and 8 summarize the parametric fits for GCR exposures and trapped radiation exposures, at solar maximum and solar minimum conditions, respectively. The parametric fits representing the 95% confidence limit on the regression fit parameters are illustrated.

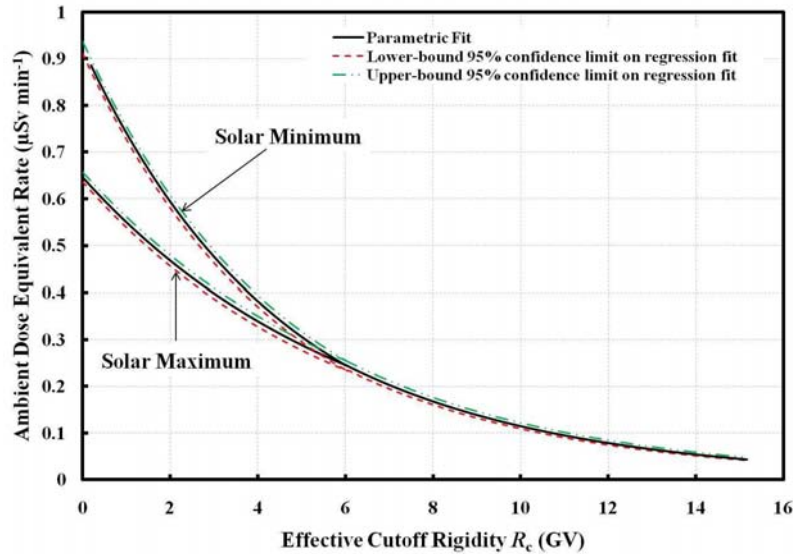


Figure 7. GCR exposure parametric fit for July 7-13, 2001 and December 10-16, 2008 TEPC data sets. For $R_c > 6.027$ GV, the parametric fits were averaged to provide a physical solution. For $R_c > 6.048$ GV, the lower-bound 95% confidence limits on the regression fits were averaged to provide a physical solution. For $R_c > 6.012$ GV, the upper-bound 95% confidence limits on the regression fits were averaged to provide a physical solution.

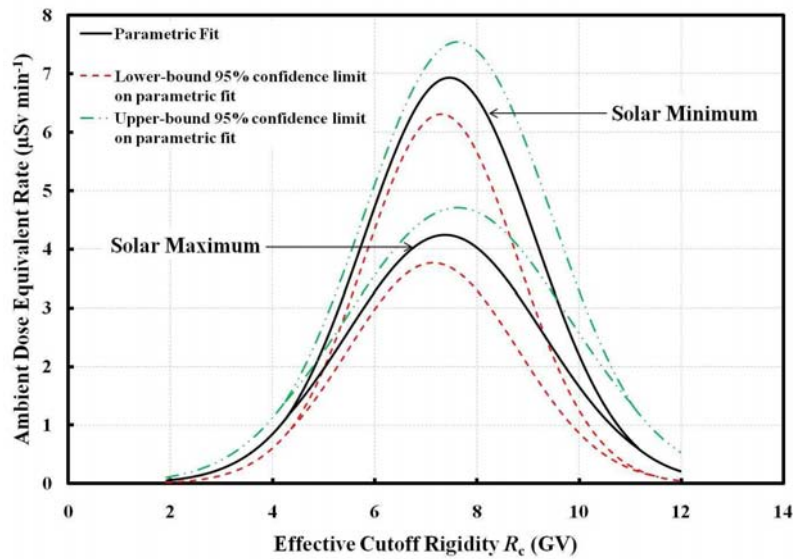


Figure 8. Trapped radiation exposure parametric fit for July 7-13, 2001 and December 10-16, 2008 TEPC data sets. For $R_c < 4.294$ GV and $R_c > 11.153$ GV, the parametric fits were averaged to provide a physical solution. For $R_c < 4.224$ GV and $R_c > 11.059$ GV, the lower-bound 95% confidence limits on the regression fits were averaged to provide a physical solution. For $R_c < 4.347$ GV and $R_c > 11.623$ GV, the upper-bound 95% confidence limits on the regression fits were averaged to provide a physical solution.

Examining Fig. 7, it is evident that near the poles where the cut-off rigidity is smallest due to the magnetic field lines being oriented towards Earth’s surface, the ambient dose equivalent rate due to GCR exposure is highest for both solar maximum and solar minimum conditions. It is also observed that during solar maximum conditions, the ambient dose equivalent rate is reduced relative to solar minimum conditions, which is expected. As the cut-off rigidity increases, thus approaching the equator where magnetic field lines run parallel to Earth’s surface, the ambient equivalent dose rates converge. This is to be expected as particles with very high rigidities are minimally affected by magnetic field conditions. Examining Fig. 8, it is again observed that solar minimum conditions result in increased dose rates relative to solar maximum conditions. These curves are valid within the SAA only.

4. Preliminary results

The parametric fits of Section 3.2, the SAA definition of Section 3.1.3, and the solar modulation parameters of Section 3.1.4 were developed into a predictive code. The code can then be benchmarked against TEPC data measured over a particular period of interest independent of those used in the model development. The state vectors tabulated for two time periods aboard the International Space Station, June 4 – 20, 2005 and April 1 – 21, 2010 in which the TEPC was placed in Service Module Panel 327 (SM-327) [18], were interpolated against the IGRF-2005 cut-off rigidity map developed by Nymmik [21]. The map was utilized since it represented the most up to date version for the time periods in question. The interpolated cut-off rigidity values were then flagged, utilizing the state vector information, as either within the SAA or out of the SAA. Given the flag type and the interpolated cut-off rigidity, the appropriate parametric fit was utilized to calculate the ambient dose equivalent rate. The corresponding state vector field was used to indicate the ISS position. The orientation of the detector as well as the condition of the environment (i.e. distribution of materials within the module) is unknown and assumed to be negligible at this time. Altitude variations and fluctuations in the cut-off rigidity, due to magnetic field fluctuations, were also ignored in the predictions. Tables 4 and 5 include the predictions for the June 4 - 20, 2005 mission and the April 1 - 21, 2010 mission, respectively. Predictions were made for each time period using the solar modulation parameters discussed in Section 3.1.4.

Table 4. Predicted ambient dose equivalent for June 4 – 20, 2005 as a function of solar modulation parameter. Bracketed values indicate the percent difference with tabulated results (Plain font for parametric fit, bold font for upper-bound 95% confidence limit on the parametric fit). Values rounded to nearest integer.

		Total Ambient Dose Equivalent	GCR Ambient Dose Equivalent	Trapped Ambient Dose Equivalent
Measured values (mrem):		777.8	532.9	244.8
Code predictions (mrem):	Solar Modulation Parameters	SSN: 923 (-19 / -26)	657 (-23 / -27)	266 (-9 / -23)
		F10.7: 899 (-16 / -23)	646 (-21 / -25)	253 (-3 / -17)
		U : 873 (-12 / -19)	634 (-19 / -23)	239 (3 / -10)

Table 5. Predicted ambient dose equivalent for April 1 – 21, 2010 as a function of solar modulation parameter. Bracketed values indicate the percent difference with tabulated results (Plain font for parametric fit, bold font for upper-bound 95% confidence limit on the parametric fit). Values rounded to nearest integer.

			Total Ambient Dose Equivalent	GCR Ambient Dose Equivalent	Trapped Ambient Dose Equivalent
Measured values (mrem):			1346.8	843.3	503.4
Code predictions (mrem):	Solar	SSN:	1146 (15 / 10)	814 (3 / 0)	332 (34 / 25)
	Modulation	F10.7:	1147 (15 / 10)	815 (3 / 0)	332 (34 / 25)
	Parameters	U :	1142 (15 / 10)	813 (4 / 1)	329 (35 / 26)

It should be noted that for the June 2005 time period, the tabulated values include five days in which the TEPC did not have full day coverage. During these five days, the TEPC provided measurements for only 94%, 99%, 97%, 93%, and 93% of the day. Therefore, the measured values are slightly less than that actually experienced. Similarly, the April 2010 time period measurements included seven days at 98%, 99%, 97%, 99%, 84%, 99%, and 99% coverage.

5. Discussion

The June 4 – 20, 2005 period represents moderate solar activity during Solar Cycle 23 while the April 1 – 21, 2010 period represents near solar minimum conditions on the ascending phase of Solar Cycle 24. It is observed that the total ambient dose equivalent predicted for both periods of time is within an absolute percent difference of 20% using parametric fit and within an absolute value of 30% when using the upper-bound 95% confidence limit on the parametric fit as a conservative estimate. The contribution to the total ambient dose equivalent from trapped radiation sources improves from a percent difference less than 40%, for the April 2010 period, to within 10% for the June 2005 period. The GCR contributions are seen to go from an under-prediction within 10%, for the April 2010 period, to an over-prediction within 25% for the June 2005 period. There is a systematic over-prediction in the June 2005 predictions and a systematic under-prediction in the April 2010 predictions. Given that the conditions used in the model best approximate the June 2005 period, it is not clear if the systematic under predictions and over predictions are a by-product of the parametric fits or of the external parameters used (i.e. SAA definition, cut-off rigidity map). Recall that the SAA map is said to be valid for an epoch spanning 2001 to 2006 [22]. In the year 2010, the SAA will have shifted in position and intensity relative to the epoch assumed.

Focusing attention to the June 2005 period, in which conditions are best approximated, it is seen that the heliocentric potential offers the most accurate approximation of the total absorbed ambient dose equivalent. Other assumptions may affect this estimate, including: (i) the use of a hard boundary for the SAA where, realistically, a penumbral region is present and (ii) ignoring altitude fluctuations which may affect the geographical limits of the SAA [12-14]. The improvements in the trapped radiation predictions from the April 2010 period to the June 2005 period suggest that the SAA has a significant impact on the quality of the predictions. The

definition of the cut-off rigidity map is also believed to have an impact. For the June 2005 time period, the IGRF-2005 map used is roughly accurate however, for the April 2010 time period, this map is less ideal. Relative to the SAA definition, however, evidence suggests that the cut-off rigidity has a less of an impact on the given predictions.

6. Conclusions

A preliminary assessment of the validity of a predictive model, utilizing as its basis a correlation between the ambient dose equivalent rate measured by the US tissue equivalent proportional counter (TEPC) and cut-off rigidity values interpolated from ISS position vectors, has yielded promising results. Utilizing TEPC data spanning six days in July 2001 to model solar maximum conditions and six days in December 2008 to model solar minimum conditions, the current work has demonstrated the ability to predict the total dose equivalent to within 20 % of the tabulated values. The accurate definition of the South Atlantic Anomaly is found to be the most significant parameter affecting the prediction.

7. Acknowledgements

The authors would like to acknowledge N. Zapp and K. Lee of the Space Radiation Analysis Group NASA for providing the TEPC data used in this analysis.

8. References

- [1] Denkins, P., Badhwar, G., Obot, V., Wilson, B., Jejelewo, O., "Radiation transport modeling and assessment to better predict radiation exposure, dose, and toxicological effects to human organs on long duration space flights", *Acta Astronautica*, Vol. 49, No. 3-10, 2001, pp. 313-319.
- [2] Johnson, A. S., Golightly, M. J., Weyland, M. D., Lin, T., Zapp, E. N., "Minimizing space radiation exposure during extra-vehicular activity", *Advances in Space Research*, Vol. 36, Issue 12, 2005, pp. 2524-2529.
- [3] Ersmark, T., Carlson, P., Daly, E., Fuglesang, C., Gudowska, I., Lund-Jensen, B., Nieminen, P., Pearce, M., Santin, G., "Geant4 Monte Carlo simulations of the belt proton radiation environment on board the International Space Station/Columbus", *IEEE Transactions on Nuclear Science*, Vol. 58, No. 4, 2007, pp. 1444-1453.
- [4] Ersmark, T., Carlson, P., Daly, E., Fuglesang, C., Gudowska, I., Lund-Jensen, B., Nieminen, P., Pearce, M., Santin, G., "Geant4 Monte Carlo simulations of the galactic cosmic ray radiation environment on-board the International Space Station/Columbus", *IEEE Transactions on Nuclear Science*, Vol. 58, No. 5, 2007, pp. 1854-1862.
- [5] "Guide to modeling Earth's trapped radiation environment", *American Institute of Aeronautics and Astronautics*, 1999.
- [6] Vanderbilt University School of Engineering, "CREME", website: <http://space-env.esa.int/ProjectSupport/ISO/CREME96.html>, 2010.

- [7] The International Association of Geomagnetism and Aeronomy, “International Geomagnetic Reference Field”, website: <http://www.ngdc.noaa.gov/IAGA/vmod/igrf.html>, 2010.
- [8] Bothmer, V. and Daglis, I., “Space Weather Physics and Effects”, *Springer*, 2007.
- [9] Lewis, B., “Review of Radiation Detector Research and Technology Development”, *Lewis Consultants (Internal Contract Report)*, 2001.
- [10] Tascione, T., “Introduction to the space environment 2nd Edition”, *Orbit*, 1994.
- [11] Lewis, B.J., “Materials and the space environments; Part I: The space environment”, *Royal Military College of Canada CME452*.
- [12] Smart, D. F., Shea, M. A., Fluckiger, E. O., “Magnetospheric Models and Trajectory Computations”, *Space Science Reviews*, 93, 2000, pp. 305-333.
- [13] Smart, D.F. and Shea, M.A., “A review of geomagnetic cutoff rigidities for earth-orbiting spacecraft”, *Advances in Space Research*, Vol. 36, 2005, pp. 2012-2020.
- [14] Smart, D. F., Shea, M. A., Tylka, A. J., Boberg, P. R., “A geomagnetic cutoff rigidity interpolation tool: Accuracy verification and application to space weather”, *Advances in Space Research*, Vol. 37, 2006, pp. 1206-1217.
- [15] Cooke, D. J., Humble, J. E., Shea, M. A., Smart, D. F., Lund, N., Rasmussen, I. L., Byrnak, B., Goret, P., Petrou, N., “On Cosmic Ray Terminology”, *Il Nuovo Cimento*, Vol. 14 C, N. 3, 1991 pp. 213-234.
- [16] Lewis, B. J., Desormeaux, M., Green, A. R., Bennet, L. G. I., Butler, A., McCall, M., Saez Vergara, J. C., “Assessment of aircrew radiation exposure by further measurements and model development”, *Radiation Protection Dosimetry*, Vol. 111, No. 2, 2004, pp. 151-171.
- [17] Lewis, B. J., Bennett, L. G. I., Green, A. R., McCall, M. J., Ellaschuk, B., Butler, A., Pierre, M., “Galactic and solar radiation exposure to aircrew during a solar cycle”, *Radiation Protection Dosimetry*, Vol. 102, No. 3, 2002, pp. 207-227.
- [18] Space Radiation Analysis Group (Private Communication).
- [19] Lewis, B., Bonin, H. W., “Health Physics and Radiation Protection, Department of Chemistry and Chemical Engineering”, *Royal Military College of Canada RMC-CCE-HWB-90-1 (Rev 1)*, 2004.
- [20] Smart, D.F., and Shea, M.A., “RCINTUT3”, (Private Communication).
- [21] Nymmik, R.A., Panasyuk, M. I., Petruckhin, V. V., Yushkov, B. Y., “A method of calculation of vertical cutoff rigidity in the geomagnetic field”, *Cosmic Research*, Vol. 47, No. 3, 2009, pp. 191-197.
- [22] Ginet, G. P., Madden, D., Dichter, B. K., Brautigam, D. H., “Energetic proton maps for the South Atlantic Anomaly”, *US Government Work Not Protected by US Copyright (Internal Manuscript)*, 2007, pp. 1-8.
- [23] National Oceanic and Atmospheric Administration National Geophysical Data Center, “Space Weather”, website: (ftp://ftp.ngdc.noaa.gov/STP/SOLAR_DATA/), 2011.
- [24] Federal Aviation Administration, “Heliocentric Potential”, website: http://www.faa.gov/data_research/research/med_humanfacs/aeromedical/radiobiology/heliocentric/, 2010.